

Internal Discontinuity Detection in Concrete by Lamb Waves

by Y.C. Jung,* T. Kundu† and M. Ehsani‡

ABSTRACT

The feasibility of detecting anomalies or discontinuities in concrete beams using lamb waves is investigated in this paper. The traditional ultrasonic methods for inspecting discontinuities in concrete use the reflection, transmission and scattering of longitudinal waves by internal discontinuities. Signal amplitude and time of flight measurements provide information about the internal anomalies in concrete. However, these methods are time consuming and, as will be shown in this paper, the traditional techniques often fail to detect honeycombs, closed cracks and small anomalies. In this paper the potential of the lamb wave technique to detect those anomalies in large concrete beams is investigated. The lamb wave technique is found to be reliable for detecting such anomalies.

Keywords: nondestructive testing, ultrasonic testing, concrete inspection, highway infrastructure, lamb waves.

INTRODUCTION

The existence of discontinuities in concrete structures is inevitable due to the low tensile strength of concrete (Park and Paulay, 1975). Invisible cracks in concrete create a major difficulty for monitoring these structures; that is, it is hard to estimate the proper time to repair, rehabilitate or strengthen the structures. There is a growing need, therefore, for nondestructive testing (NDT) techniques to assess the condition of concrete structures, predict their future performance and monitor the repair process.

In spite of a number of NDT methods with sophisticated techniques available today, very few techniques are applicable for inspecting concrete structures efficiently. If applied properly, NDT can make a significant contribution towards evaluating and monitoring building safety as well as further developing construction technology. In addition, the ability to determine the anomalies of concrete structures *in situ* using NDT techniques is gaining popularity. The techniques that are currently used are primarily destructive and may require random coring, drilling or otherwise removing part of the structure for testing. Some of the proposed NDT techniques are also cumbersome and require sophisticated equipment. The technique presented in this paper gives an efficient NDT method to detect internal damage in concrete structures.

NDT OF CONCRETE

In spite of recent developments in testing techniques and equipment, the use of NDT for testing concrete poses many difficulties. Compared to NDT of metal and metal based materials, NDT of concrete is a relatively immature discipline. The heterogeneous nature of concrete and the lack of a universally accepted technique for the NDT of concrete are two main reasons why concrete testing technology lags behind that for structural metals.

Concrete is a multiphase material consisting of coarse aggregate comprising particles of more than 5 mm (0.2 in.) in diameter, fine aggregate, sand and cement. The coarse granular structure, such as

the relative concentration of the constituent particles, the degree of compaction, the moisture content and the nature and amount of anomalies present, gives rise to a high degree of acoustic scattering and, therefore, attenuation. For this reason, testing is usually done at kilohertz frequency range. In addition, the presence of steel rods gives rise to more complications for testing of reinforced concrete.

It is well known that there are existing codes or standards available to be used as guidelines for construction materials other than concrete. For instance, the American Society of Mechanical Engineers (ASME) code is commonly used for construction of boilers and pressure vessels, the American Petroleum Institute (API) code for construction in the petroleum industry and the American Welding Society (AWS) code for the construction of steel structures. In such cases, the application of NDT is well specified. However, for civil construction involving concrete, there is no specific code or standard currently available that can be used as a guideline for the selection and application of suitable NDT methods or for the acceptance and rejection criteria. Due to these facts, the NDT community should have a wide knowledge of NDT applications, so that the appropriate NDT technique can be selected for use in a particular situation.

Concrete experts have been interested in detecting internal anomalies and determining the properties of concrete by NDT techniques for many decades and a number of NDT techniques have been used for concrete testing. However, the visual testing technique is still the most popular technique. Eighty percent of anomalies in concrete are found by visual inspections (Bray and Stanley, 1997). Among more advanced techniques, the ultrasonic pulse velocity technique has been standardized (ASTM C597-83). Advantages and disadvantages of this technique have been discussed by a number of researchers (Schickert and Wiggerhauser, 1995; Jones, 1962; Malhotra and Carino, 1991; Popovics, 1994). Impact echo is also a popular ultrasonic technique for concrete testing (Krause et al., 1995; Pessiki and Johnson, 1994; Sansalone and Strett, 1997). Other NDT techniques that have been used for concrete testing include acoustic emission, thermographic imaging, ground penetrating radar, laser interferometry, falling weight deflectometer and laser profilometer.

A BRIEF REVIEW OF LAMB WAVES

Lamb waves, also known as guided plate waves, are elastic stress waves that are observed in plates. They are guided by the plate surface boundary, which acts as a waveguide. In other words, waves that propagate in a plate and satisfy the plate boundary conditions at both surfaces of the plate are known as lamb waves. There are an infinite number of lamb wave modes that could vibrate a plate. Different lamb modes can be generated by changing the signal frequency and the incidence angle of the transmitter. In a homogeneous plate these modes can be classified into two main groups, according to the direction of the particle displacement: symmetrical and antisymmetrical modes. The wave velocity depends on the plate thickness, the frequency, the mode order and the material properties.

Lamb waves propagate dispersively in the plane of the plate through the entire cross section. Lamb waves can also be launched in curved plates and pipes. Cylindrical lamb waves (or cylindrical guided waves) propagate along a pipe. This technology is being exploited by investigators to detect anomalies in pipes (Silk and Bainton, 1979; Avioli, 1988; Rose et al., 1996; Guo and Kundu, 1998; Guo and Kundu, 2000).

* Department of Civil Engineering and Engineering Mechanics, the University of Arizona, Tucson, AZ 85721; e-mail <yjung@email.arizona.edu>.

† Department of Civil Engineering and Engineering Mechanics, the University of Arizona, Tucson, AZ 85721; e-mail <tkundu@email.arizona.edu>.

‡ Department of Civil Engineering and Engineering Mechanics, the University of Arizona, Tucson, AZ 85721; e-mail <ehsani@email.arizona.edu>.

Adv
W
area
by th
cause
that i
point
deper
ceivin
nals t
the tw
test a
TH
lamb
shape
of ind
shoul
ble to
plate
mode
er me
De
based
the d
small
anom
used
for de
deper
on ho
fects

Figure

Advantages of Using Lamb Waves

With the conventional ultrasonic methods mentioned above, the area under interrogation at any instant is limited to the region covered by the transducer. As a result, this method is very time consuming because the transducer must be placed over every point of the structure that is to be tested. In contrast, the lamb wave can be excited at one point of the structure and can propagate over a considerable distance depending on the wavelength. With the pitch catch arrangement, a receiving transducer kept at a distance can pick up the propagating signals that contain information about the integrity of the region between the two transducers. Therefore, the lamb wave testing technique can test a comparatively large region in a short time.

The entire thickness of the plate can be inspected by different lamb modes exciting different depths of the plate. From the mode shapes (stress and displacement profiles across the plate thickness) of individual lamb modes one can conclude which lamb mode should be sensitive to what depth of the plate. This makes it possible to detect anomalies near the surface as well as those inside the plate. Since each mode has its own mode shape, sensitivity of one mode to a specific anomaly at a depth will vary from that of another mode that has a different mode shape.

Detection of anomalies by conventional ultrasonic methods is based on the principle of ultrasound being reflected or scattered by the discontinuities. Therefore, the wavelength determines the smallest size anomaly that can be detected by a certain signal. Small anomalies are difficult to detect by signals of the low frequencies used for concrete testing. The lamb wave method is very promising for detecting small anomalies because anomaly detection does not depend only on the reflection of the waves from discontinuities, but on how the waves interact with them. This important interaction affects the voltage amplitude versus frequency $V(f)$ curves in two

ways. The peak amplitude corresponding to a particular mode may change because of the presence of a discontinuity or there may be a frequency shift of the peak amplitude. These were used by Mustafa et al. (1996) to image disbands in the tear strap in the pitch catch arrangement with the angle wedge transducers.

In summary, lamb waves are used because they offer an improved testing potential due to their multimode characteristics, sensitivity to different types of discontinuities, propagation over long distances, guiding character that enables them to follow curvature and reach hidden or buried parts and the capability of *in situ* testing.

EXPERIMENTAL INVESTIGATION

Under this investigation a number of specimens have been fabricated and tested by different lamb modes. The first step of lamb wave testing is to produce lamb waves inside the specimen. To this aim two transducers of 50 kHz resonance frequency are placed over an anomaly free plate specimen. The transmitter is excited by a continuous wave or tone burst signal. The generated signal is amplified and then used for exciting the transmitter. The signal frequency is continuously varied between 25 and 200 kHz. The receiving transducer receives the signal after its propagation through the specimen. The received signal amplitude is then displayed on an oscilloscope screen as a function of frequency. The gate position is placed near the beginning of the received signal (the "gate" represents the time window for the received signal used to generate the $V(f)$ curve). This is done to avoid collecting signals after those are reflected by other boundaries. Therefore, the early part of the received signal should be affected by the presence of the anomaly. The experimental setup is similar to the one developed by Ghosh and Kundu (1998) and Ghosh et al. (1998) and is shown in Figure 1.

Kundu et al. (1996), Maslov and Kundu (1997) and Yang and

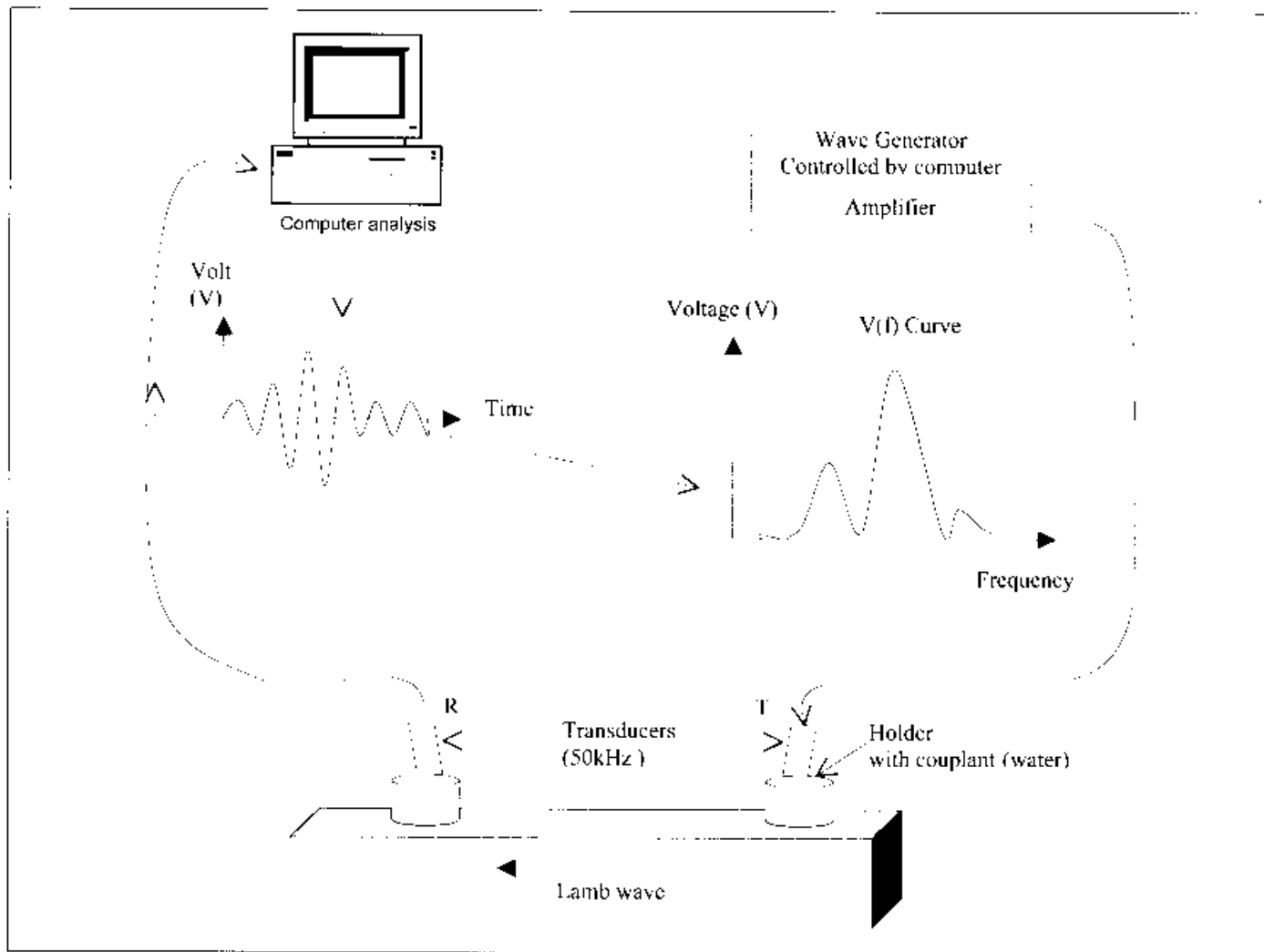


Figure 1 — Schematic of the experimental setup.

did not
cate the
gate size

The
men on
electric
hand sig
cylinder
placed a
concrete
concrete
second
anomal
vibrated

Speci
placed s
and typ
ricated b
m (5.9 b
(5.1 by 9
specime
they wo
twenty
tered at
mens w
to meas
from the
are show

V(f) Curves

Vari
nal freq
curves a
curves v
constant
receiver
transmit
crete bea
the trans
ized lam
nities. S
transmis
continui

EXPERI

Through

V(f) c
techniqu
placing t
faces of
are place

Different dips along the frequency axis are observed when the transducer angle is changed because of the generation of different lamb modes. In this manner, by monitoring the transducer angles and dips of the reflected signal spectra, the lamb wave dispersion curves can be experimentally generated. For testing a plate with lamb waves, the transducer angle (θ) is set by selecting a specific lamb mode for testing. Then the transducer is placed and excited in the tone burst mode.

Finally, the signal frequency is set at a value corresponding to a lamb mode of interest. The specimen is then inspected with this transmitter receiver arrangement.

P- and S-wave Speed Measurement in Concrete

During concrete testing, low frequency waves should be used to decrease the attenuation of wave energy due to scattering at the mortar aggregate interfaces. If the wavelength of the propagating wave is less than the maximum size of the aggregate, the aggregate causes undesirable scattering of waves at mortar aggregate interfaces. As a result, a low frequency signal is needed for concrete testing. For example, when the maximum aggregate size is 10 mm (0.4 in.) in concrete and its P-wave speed is 4 km/s (2.5 mi/s), frequencies lower than $4/0.01 = 400$ kHz should be used to reduce scattering and attenuation. The concrete appears homogeneous to the low frequency waves (Sansalone and Carino, 1991).

The P- and S-wave speeds in concrete can be measured experimentally. The direct through transmission measurement was used for determining the P-wave speed. The S-wave speed was then obtained using the expression of the S-wave speed in terms of the Poisson's ratio and P-wave speed,

$$(2) \quad V_s = V_p \sqrt{\frac{1-2\nu}{2(1-\nu)}}$$

In our experiment the signal wavelengths for P-waves in the frequency range between 53 and 116 kHz is between 76 mm and 35 mm (3 and 1.4 in.), that is, much larger than the aggregate size of 10 mm (0.4 in.). For a lamb wave speed of 5.41 km/s (3.4 mi/s), for the transducer inclination angle of 16 degrees, the signal wavelength is even larger. As a result, wave scattering at the interfaces between the aggregate particles and mortar is negligible. In addition, the acoustic impedance of aggregate and that of the mortar are very close; this further reduces the scattering at the mortar aggregate interface.

Sample Preparation

Two types of beam specimens measuring 1 by 0.3 by 0.2 m (39.4 by 11.8 by 7.9 in.) with different types of anomalies in various locations were cast. Each type was cast in duplicate. Internal anomaly geometry and location in the concrete beam are shown in Figure 3. The specimens are denoted as specimens one and two. Specimen one contained no anomaly on the left hand side. The signal from this region is denoted as the reference signal or anomaly free signal. On the right hand side, specimen one included a honeycomb anomaly. Specimen two contains an acrylic inclusion and a crack on the left and right hand sides, respectively. These concrete specimens

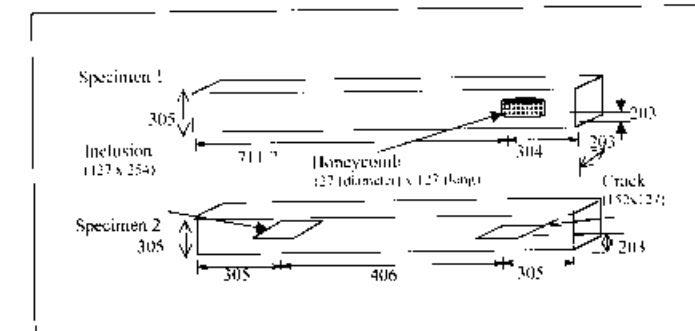


Figure 3 — Geometry of concrete beams and internal anomaly positions (lengths given in millimeters).

Kundu (1998) investigated the reflected wave spectra for different transmitter receiver specimen orientations. They have shown that when the transmitter and the receiver are positioned such that the reflected energy is maximized or is very close to the maximum, then the reflected amplitude spectrum should have a shape similar to that shown in Figure 2a or 2b. Signal amplitudes have been normalized with respect to the maximum values. If no lamb waves are generated in the specimen, the spectrum has no dips, as shown in Figure 2a. However, dips are observed if lamb waves are generated, as shown in Figure 2b. When the specimen is immersed in water, the lamb wave energy is leaked into the water; that is why they are also called leaky lamb waves. When transducers are defocused, or, in other words, the transducers are moved closer to the specimen, then the reflected amplitude spectrum changes its shape and magnitude. Note that for the relative orientations of transducers and plate shown in Figure 2b the receiver receives the direct or spectrally reflected signal; we call this position the focused position. If the specimen moves closer to the transducers, as shown in Figure 2c, then the position is called defocused position. In this defocused position, peaks, instead of dips, are observed at the frequencies at which lamb waves are generated. Because of high defocusing, the specularly reflected beam cannot reach the receiver but the leaky lamb waves can. That is why we observe peaks in Figure 2c when lamb waves are generated. The frequencies corresponding to the lamb modes can be obtained from either the dips or peaks. The lamb wave phase velocity (V_{ph}) can be obtained from Snell's Law,

$$(1) \quad V_{ph} = \frac{\alpha_w}{\sin \theta}$$

where

- V_{ph} = the lamb wave phase velocity
- α_w = the longitudinal wave speed in the couplant fluid (for water it is equal to 1.49 km/s [0.9 mi/s])
- θ = the angle of inclination of the transducer, that is, the angle between the vertical axis and the transducer axis.

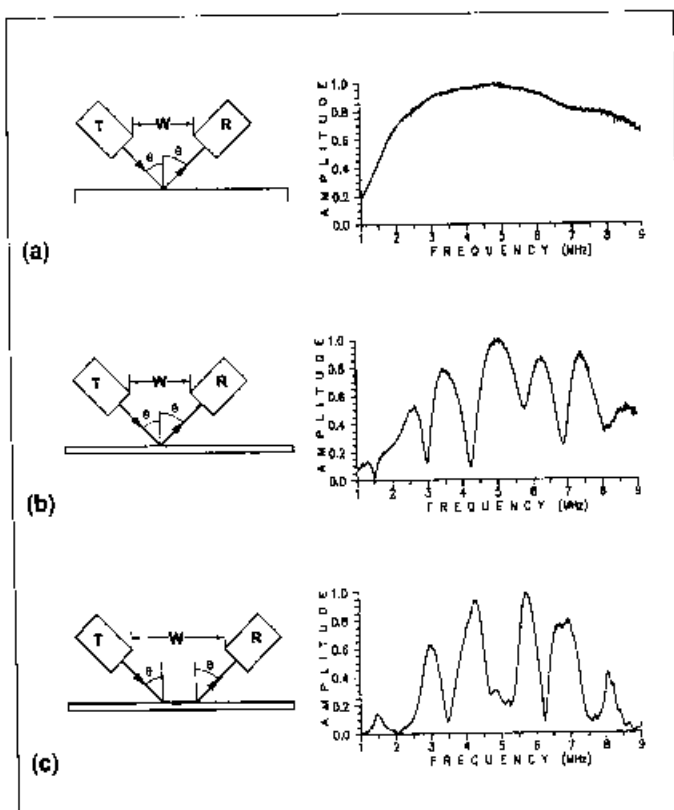


Figure 2 — (a) V(f) curve when no lamb wave is generated; (b) when lamb waves are generated in the focused position; (c) when lamb waves are generated in the defocused position (Kundu et al., 1996).

Table 1 Proportions of concrete mix used to fabricate the beams

Ingredient	Amount	Ingredient Description	Mix Ratio
Cement	298.5 kg (658 lb)	Low alkali	0.166
Water	140.5 kg (310 lb)		0.078
Sand	624.5 kg (1377 lb)	Standard surface dry	0.348
Rock	728.5 kg (1606 lb)	10 mm (0.4 in.) maximum size	0.406
Water reducer	1.2 kg/m ³ (0.07 lb/ft ³)	WRDA-64	0.002
Total	1792.0 kg (3951 lb)	Standard mix	1.000

Table 2 Material properties of concrete cylinders

Material Properties	Specimen 1	Specimen 2	Specimen 3
P-wave speed in km/s (mi/s)	4.02 (2.498)	4.06 (2.523)	4.03 (2.504)
Poisson's ratio	0.22	0.24	0.19
S-wave speed in km/s (mi/s)	2.40 (1.49)	2.38 (1.48)	2.49 (1.55)
Density in kg/m ³ (lb/ft ³)	2195.0 (137)	2160.0 (135)	2186.0 (136)
Young's modulus in kg/m ² (lb/ft ²)	2.30×10^9 (4.71×10^8)	2.29×10^9 (4.69×10^8)	2.45×10^9 (5.02×10^8)

did not have any reinforcement. Proportions of mixes used to fabricate the beams are summarized in Table 1. The maximum aggregate size was 10 mm (0.4 in.).

The concrete beam specimens were cast in wood forms. Specimen one was filled in three layers. Each layer was vibrated with an electric vibrator. The simulated anomaly was placed on the right hand side of the beam. When the first layer was vibrated, a plastic cylinder 0.13 m (5 in.) in diameter and 0.25 m (10 in.) long was placed and filled with only aggregates (same size aggregates as the concrete mix but without any mortar). Then the second layer of concrete was placed and the plastic cylinder was removed after the second layer had been vibrated. In this manner a honeycomb anomaly zone was fabricated. Finally, the third layer was cast and vibrated.

Specimen two was cast in two layers. The simulated cracks were placed slightly above the midplane. Simulated anomaly positions and types are summarized in Figure 3. The artificial crack was fabricated by placing a water filled sealable bag measuring 0.15 by 0.13 m (5.9 by 5.1 in.) inside the concrete. A 0.13 m by 0.25 m by 3 mm (5.1 by 9.8 by 0.1 in.) acrylic sheet was cast near the left end of the specimen to represent an inclusion. After the specimens were cast, they were cured under plastic sheets to minimize moisture loss. Twenty four hours after casting, the beams were stripped and watered at regular intervals for 28 days. While casting the two specimens with internal anomalies, three more cylinders were also cast to measure the concrete properties. Concrete properties measured from these three cylinders by the standard 28 day compression test are shown in Table 2.

V(f) Curve

Variation of the received signal voltage as a function of the signal frequency is denoted as the $V(f)$ curve. Changes in the $V(f)$ curves are caused by the internal anomalies. A number of $V(f)$ curves were generated in the same region of the beams, keeping a constant distance of 0.2 m (7.9 in.) between the transmitter and the receiver to study the repeatability of the experiment. When both the transmitter and receiver are located on the same surface of the concrete beam (Figure 1), then generalized lamb waves propagate from the transmitter to the receiver. $V(f)$ curves generated by the generalized lamb waves show good consistency and sensitivity to discontinuities. Similar $V(f)$ curves generated by the conventional through transmission technique lack both consistency and sensitivity to discontinuities.

EXPERIMENTAL RESULTS

Through Transmission Technique

$V(f)$ curves generated by the conventional through transmission technique are shown in Figure 4. These curves are generated by placing the transmitter and the receiver on the top and bottom surfaces of the specimens shown in Figure 3. Hence, the transducers are placed 0.3 m (12 in.) apart facing each other and the specimen is

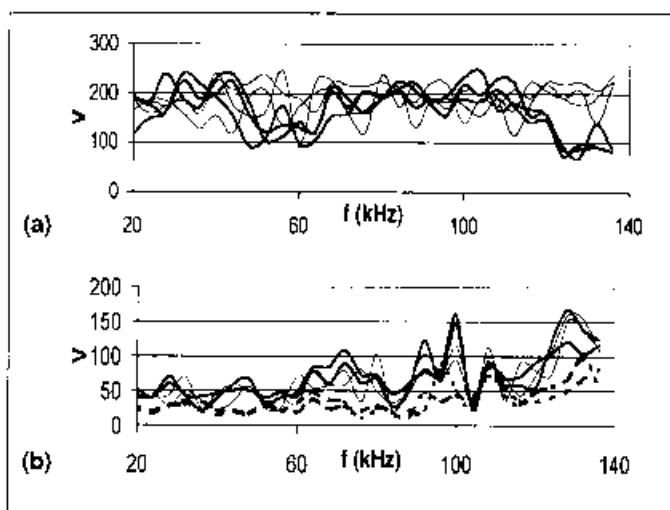


Figure 4 — Voltage versus frequency curves generated by the conventional through transmission technique for (a) specimen one and (b) specimen two. Signals from the anomaly free zone are shown by thin lines in both. Signals from the honeycomb zone are shown by thick lines in (a); signals from the zone containing the inclusion are shown by the continuous thick lines in (b) and the dotted lines represent the signals from the cracked zone.

in between the two transducers. A thin film of petroleum jelly was used over the contact area between the transducers and the specimen. Figures 4a and 4b show some difference between the $V(f)$ curves generated by the defective and nondefective zones. However, the curves are not consistent and the difference is not very clear. Only the cracked zone gives a noticeably weaker signal than the anomaly free zone (Figure 4b). Signals from the zones containing the honeycomb and the inclusion anomalies are very close to those from the anomaly free region.

Lamb Wave Technique

The $V(f)$ curves generated by the generalized rayleigh-lamb waves are shown in Figures 5, 6 and 7 for both defective and nondefective zones. One can see the noticeable difference between the $V(f)$ curves from the defective and defect free zones, unlike the $V(f)$ curves of Figure 4, obtained from the through transmission testing.

Experimental Results for Specimen One

$V(f)$ curves for both anomaly free and honeycomb regions of specimen one are shown in Figure 5. The transducers were inclined at an angle of 16 degrees. This inclination angle corresponds to a phase velocity of 5.41 km/s (3.4 mi/s [see Equation 1]). The $V(f)$ curve for the 16 degree angle of incidence was generated several times to study the consistency of the results. Two

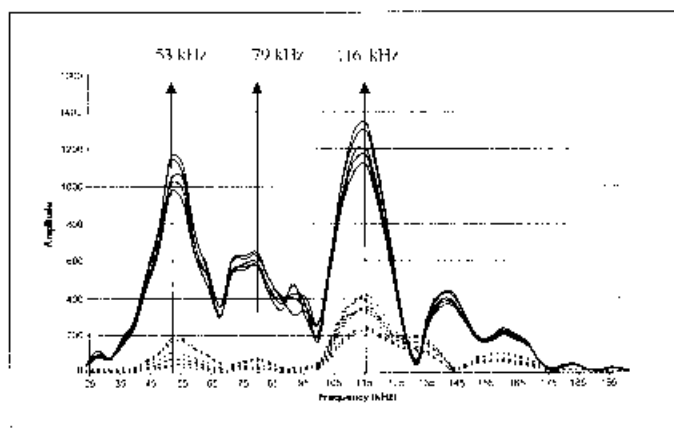


Figure 5 — $V(f)$ curves over nondefective zone (continuous lines) and honeycomb region (dotted lines).

strong distinguishing peaks are observed, one near 53 kHz and the one near 116 kHz. The wavelengths corresponding to these two lamb modes are 0.1 m and 47 mm (3.9 and 1.9 in.) respectively. Clearly the maximum aggregate size of 10 mm (0.4 in.) is much smaller than the wavelength. More peaks near 79, 145, 160, 180, 200 and 28 kHz are also observed in the $V(f)$ plot, however, these peaks are much weaker than the peaks at 53 and 116 kHz.

Fewer and weaker peaks are observed over the honeycomb region. Prominent peaks are again noticed at 53 and 116 kHz. Weaker peaks are observed near 80 and 160 kHz. This comparison of $V(f)$ curves clearly shows that the amplitudes of the signal are significantly reduced by the existence of the honeycomb inside the specimen. However, the positions of the prominent peaks were not changed by the presence of the honeycomb. The reason behind the amplitude reduction is that the generated lamb waves cannot travel through the air gaps present in the honeycomb zone.

These results are similar to Jones's (1962) observation of longitudinal wave propagation in concrete; that although quite large internal voids may produce relatively small decreases in the effective pulse velocity, they obstruct the direct energy and cause a considerable reduction in the amplitude of the received pulse. It is for this reason that even an approximate measure of the amplitude of the received pulse is often of value in detecting the presence of voids.

Experimental Results for Specimen Two

For specimen two, two prominent peaks near 53 and 116 kHz are observed and shown in Figure 6. These peak positions are identical to those for specimen one. Weaker peaks are observed near 28, 79, 96, 150 and 172 kHz. The positions of the prominent peaks do

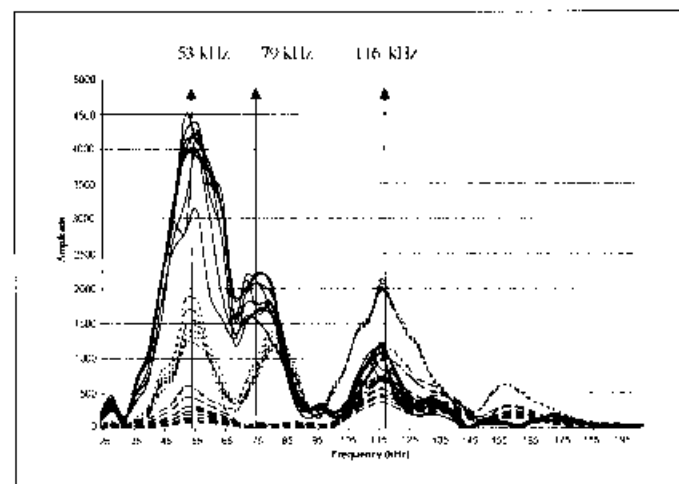


Figure 6 — $V(f)$ curves over the nondefective zone (continuous); region containing the acrylic inclusion (dotted); and the cracked region (dashed).

not change in the presence of discontinuities, but their amplitudes do. Another significant observation in this figure is that the crack gives a greater change in amplitude than the acrylic inclusion. The crack also gave a larger change of $V(f)$ in the through transmission testing (Figure 4b).

It is interesting to note that the peak near 79 kHz is strongest for the acrylic inclusion, weak but detectable for the honeycomb inclusion and almost nonexistent for the crack. It should be also noted here that while discontinuities reduce the strength of most lamb modes, peak values corresponding to few other modes in fact increase in the presence of discontinuities, indicating that the geometry changes due to the presence of discontinuities help the propagation of some lamb modes.

$V(f)$ Curves for the Normal Incidence

The purpose of this testing is to show how an inclined transducer position can significantly improve the lamb wave testing. This testing was carried out in the anomaly free and honeycomb zones of specimen one using both water and petroleum jelly as the coupling medium. The experiment was repeated several times to see the consistency of the experimental results.

Normal Incidence with Water Coupling

Generated $V(f)$ curves are shown in Figure 7. Only one prominent peak near 53 kHz is observed. The peak amplitude is significantly affected by the existence of the honeycomb anomaly.

Normal Incidence with Petroleum Jelly Coupling

Figure 8 shows $V(f)$ curves over honeycomb and anomaly free zones when petroleum jelly is used as the couplant. The experiments were carried out several times. Clearly, the difference

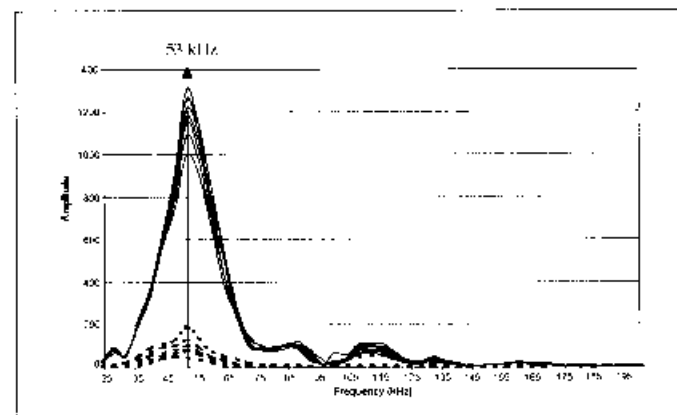


Figure 7 — $V(f)$ curves for transducers placed normal to the specimen surface with water used as the couplant; the continuous curves signify the anomaly free zone, the dashed curve represents the honeycomb zone.

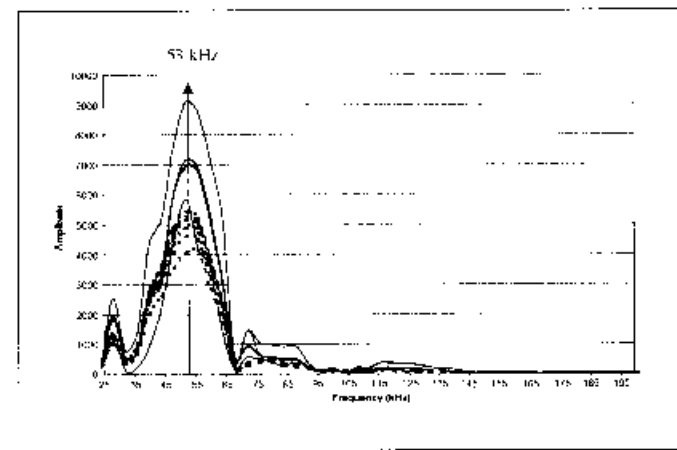


Figure 8 — $V(f)$ curves over the nondefective zone (continuous) and honeycomb zone (dotted) when the transducers are in direct contact with the specimen. Petroleum jelly is used as the couplant.

between the $V(f)$ curves for defective and nondefective zones are much less prominent in this case. This is due to the fact that the applied pressure between the transducer and the specimen affects the received voltage amplitude when petroleum jelly is used as the couplant. This is not the case for water coupling. As a result, fluctuations in the peak amplitude value are considerably greater when petroleum jelly was used as the coupling agent.

CONCLUSION

The main objective of this investigation was to study if lamb waves can detect internal anomalies in large concrete beams. The experimental results show that it is possible to detect such anomalies. Three types of anomalies — honeycombs, acrylic inclusions and cracks — have been successfully detected by the lamb wave technique. Superiority of the lamb wave technique over the conventional ultrasonic technique has been also demonstrated.

It is also shown that water coupling gives better results than petroleum jelly coupling and that the inclined transducer position is more efficient than the vertical position.

ACKNOWLEDGMENTS

This research was financially supported by the National Science Foundation under contracts number CMS-9800345 and CMS-9896182 and EPRI grants W08031-14 and EP-P241/CH10. The views presented are those of the writers and do not necessarily represent the views of the funding agencies. The writers would like to acknowledge the experimental help provided by P. Karpur of Allied Signal during this investigation.

REFERENCES

American Society for Testing and Materials, *Standard Test Method for Pulse Velocity through Concrete*, C597-83, West Conshohocken, Pennsylvania, ASTM, 1991.

Avioli, M., "Lamb Wave Inspection for Large Cracks in Centrifugally Cast Stainless Steel," Research Report to EPRI by Georgetown University, 1988.

Bray, D.F. and R.K. Stanley, *Non Destructive Evaluation*, London, CRC Press, 1997.

Ghosh, T. and T. Kundu, "A New Transducer Holder Mechanism for Efficient Generation and Reception of Lamb Modes in Large Plates," *Journal of the Acoustical Society of America*, Vol. 104, 1998, pp. 1498-1502.

Ghosh, T., T. Kundu and P. Karpur, "Efficient Use of Lamb Modes for Detecting Defects in Large Plates," *Ultrasonics*, Vol. 36, 1998, pp. 791-801.

Guo, D. and T. Kundu, "Special Sensors for Generating Lamb Waves in Pipes," *Proceedings of the Review of Progress in Quantitative Nondestructive*

Evaluation, Ed. D.O. Thompson and D.E. Chimenti, Vol. 18, New York, Plenum Press, 1998.

Guo, D. and T. Kundu, "A New Sensor for Pipe Inspection by Lamb Waves," *Materials Evaluation*, Vol. 58, No. 8, August 2000, pp. 991-994.

Jones, R., *Non Destructive Testing of Concrete*, Cambridge, Cambridge University Press, 1962.

Krause, M., H. Wiggenhauser, O. Barmann, K. Langenberg, R. Frielinghaus, F. Wollbold and M. Schichert, "Comparison of Pulse-Echo Methods for Testing Concrete," *Proceedings of the International Symposium on Nondestructive Testing in Civil Engineering (NDT-CE)*, Vol. 1, Berlin, Germany, DGZFB, 1995, pp. 281-296.

Kundu, T., K. Maslov, P. Karpur, T.E. Matikas and P.D. Nicolaou, "A Lamb Wave Scanning Approach for Mapping of Defects in [0/90] Titanium Matrix Composites," *Ultrasonics*, Vol. 34, 1996, pp. 43-49.

Malhotra, V.M. and N.J. Carino, *CRC Handbook on Nondestructive Testing of Concrete*, London, CRC Press, 1991.

Maslov, K. and T. Kundu, "Selection of Lamb Modes for Detecting Internal Defects in Composite Laminates," *Ultrasonics*, Vol. 35, 1997, pp. 141-150.

Mustafa, V., A. Chahbaz, D.R. Hay, M. Brassard and S. Dubois, "Imaging of Disbonds in Adhesive Joints with Lamb Waves," *Nondestructive Evaluation of Materials and Composites*, Vol. 2944, December 1996, pp. 87-97.

Park, R. and T. Paulay, *Reinforced Concrete Structures*, John Wiley & Sons, New York, 1975.

Pessaki, S. and M. Johnson, "Nondestructive Determination of Concrete Strength in Plate Structures by the Impact Echo Method," *Review of Progress in Quantitative Nondestructive Evaluation*, Vol. 13, 1994, pp. 2139-2146.

Popovics, J.S., "Some Theoretical and Experimental Aspects of the Use of Guided Waves for the Nondestructive Evaluation of Concrete," PhD dissertation, The Pennsylvania State University, 1994.

Rose, J.L., D. Jiao and J. Spanner, "Ultrasonic Guided Wave NDE for Piping," *Materials Evaluation*, Vol. 54, 1996, pp. 1310-1313.

Sansalone, M.J. and N.J. Carino, "Stress Wave Propagation Methods," *CRC Handbook on Nondestructive Testing of Concrete*, London, CRC Press, 1991, pp. 275-303.

Sansalone, M.J. and W.B. Strett, *Impact-Echo: Nondestructive Evaluation of Concrete and Masonry*, Ithaca, Bullbrier Press, 1997.

Schückerl, G. and H. Wiggenhauser, "Comparison of DIN / ISO 8047 (Ertwurf) to Several Standards on Determination of Ultrasonic Pulse Velocity in Concrete," *Proceedings of the International Symposium on Nondestructive Testing in Civil Engineering (NDT-CE)*, Vol. 2, Berlin, Germany, p. 1346.

Silk, M.G. and K.F. Bainton, "The Propagation of Ultrasonic Wave Mode Equivalent to Lamb Waves in Metal Tubing," *Ultrasonics*, Vol. 17, 1979, pp. 11-19.

Yang, W. and T. Kundu, "Guided Waves in Multilayered Plates for Internal Defect Detection," *ASCE Journal of Engineering Mechanics*, Vol. 123, 1998, pp. 311-318.